Impact of trace metal concentrations on coccolithophore growth and morphology: laboratory simulations of Cretaceous stress.

Giulia Faucher[1], Linn Hoffmann[2], Lennart T. Bach[3], Cinzia Bottini[1], Elisabetta Erba[1], Ulf Riebesell[3]

[1] Earth Sciences Department "Ardito Desio", Università degli Studi di Milano, Milan, Italy

5 [2] Department of Botany, University of Otago, Dunedin, New Zealand

[3] Biological Oceanography, GEOMAR Helmholtz Centre for Ocean Research Kiel, Kiel, Germany

Correspondence to: Giulia Faucher (giulia.faucher@unimi.it)

10 **Abstract.** The Cretaceous ocean witnessed intervals of profound perturbations such as volcanic input of large amounts of CO_2, anoxia, eutrophication, and introduction of biologically relevant metals. Some of these extreme events were characterized by size reduction and/or morphological changes of a few calcareous nannofossil species. The correspondence between intervals of high trace metal concentrations and coccolith dwarfism suggests a negative effect of these elements on nannoplankton biocalcification processes in past oceans. In order to test this hypothesis, we explored the potential effect of a mixture of trace

15 metals on growth and morphology of four living coccolithophore species, namely *Emiliania huxleyi, Gephyrocapsa oceanica, Pleurochrysis carterae* and *Coccolithus pelagicus*. The phylogenetic history of coccolithophores shows that the selected living species are linked to Mesozoic species showing dwarfism under excess metal concentrations. The trace metals tested were chosen to simulate the environmental stress identified in the geological record and upon known trace metal interactions with living coccolithophore algae.

20 Our laboratory experiments demonstrated that elevated trace metal concentrations, similarly to the fossil record, affect coccolithophore algae size and/or weight. Smaller coccoliths were detected in *E. huxleyi* and *C. pelagicus,* while coccoliths of *G. oceanica* showed a decrease in size only at the highest trace metal concentrations. *P. carterae* coccolith size was unresponsive to changing trace metal concentrations. These differences among species allow to discriminate most- (*P. carterae*), intermediate- (*E. huxleyi* and *G. oceanica*), and least- (*C. pelagicus*) tolerant taxa. The fossil record and the

25 experimental results converge on a selective response of coccolithophores to metal availability.

These species-specific differences must be considered before morphological features of coccoliths are used to reconstruct paleo-chemical conditions.

1 Introduction

Trace metal concentrations influence the productivity and species composition of marine algae communities (Bruland et al., 1991; Sunda and Huntsman, 1998). A number of trace metals are important micronutrients (e.g. zinc, iron, copper, nickel) but some of them can become toxic and inhibit marine algal productivity at elevated concentrations (Brand et al., 1986; Sunda and Huntsman, 1992). Others like lead and mercury have no known metabolic functions and can hamper marine phytoplankton growth already at low concentrations (Sunda, 1989; Sunda et al., 2005).

The geological record offers the opportunity to investigate past case histories marked by profound changes in the ocean, such as volcanic injection of large amounts of CO_2, ocean anoxia, eutrophication and introduction of biologically relevant metals (e.g. Larson and Erba, 1999; Erba, 2004; Jenkyns, 2010; Erba et al., 2015). These events can be seen as "natural experiments" useful to decrypt the ecosystem response to major perturbations at time scales longer than current modifications. Finding out how the changes in seawater composition affect marine biota requires the integration of a long–term and large–scale geological perspective that has been recognized as an essential ingredient for more coherent predictions of how marine organisms might react to future environmental changes. Insights on ocean/atmosphere dynamics under warmer-than-present-day conditions predicted for the end of this century can be obtained by including geological data of past ecosystems, especially those derived from cases of extreme conditions. Well-known perturbations were the "Oceanic Anoxic Events" (OAEs) which took place during the Mesozoic. These events were caused by intense volcanism that produced large igneous provinces (LIPs) (Snow et al., 2005; Neal et al., 2008; Pearce et al., 2009; Erba et al., 2015) that released magmatic fluids delivering metals, mixed with warmed ambient seawater that had enough buoyancy to rise to the surface (Snow et al., 2005; Erba et al., 2015). During the latest Cenomanian OAE 2 for example, less volatile elements, such as nickel and iron (released during the formation of the Caribbean LIP), increased by 8-20 times above seawater background levels while more volatile elements like lead and cadmium (derived from water-rock exchange reactions), increased by about 4-8 times above background level (Orth et al., 1993; Snow et al., 2005). Entering the ocean environment, more and less volatile elements became biologically relevant as evidenced by changes and turnover in marine plankton communities (Leckie, 1985; Leckie et al., 1998; Erba, 2004; Erba et al., 2015).

Studies on calcareous nannofossils documented a size reduction of some coccolithophore species (*Biscutum constans*, *Zeugrhabdotus erectus* and *Discorhabdus rotatorius*) coeval with trace metal concentration peaks across both the early Aptian OAE 1a and latest Cenomanian OAE 2 (Erba et al., 2015; Faucher et al., 2017). The fossil record shows that, although most of the Mesozoic nannoplankton taxa didn't survive the mass extinction event at the end of the Cretaceous, reconstructed phylogenetic trees (Bown et al., 2004), based on morphological observations of coccolith (shape and ultrastructure), and molecular trees, mostly based on rDNA (de Vargas and Probert, 2004) indicate a link between selected Mesozoic groups and some living coccolithophores. The group to which the four species tested here, namely *Emiliania huxleyi, Gephyrocapsa oceanica, Coccolithus pelagicus* and *Pleurochrysis carterae,* belong to, evolutionarily diverged from one another since the Late Cretaceous, with the exception of *E. huxleyi* and *G. oceanica* that are separated since 250,000 years ago (De Vargas et

al., 2007; Liu et al., 2010). Specifically, genera *Emiliania* and *Gephyrocapsa* belong to the Cenozoic family Noelaerhabdaceae derived from the extinct Prinsiaceae that, in turn, branched off the Mesozoic family Biscutaceae. Indeed, coccolith dwarfism was observed in genus *Biscutum* during times of high CO_2 and metal concentrations in both OAE 1a and OAE 2 (Erba et al., 2010; Faucher et al., 2017). It is challenging to unambiguously disentangle the cause/s of such changes in the fossil record but evidence of a correspondence between intervals of high trace metal concentrations and coccolith dwarfism suggest a negative effect of these elements on nannoplankton biocalcification processes.

Previous work on the response of living coccolithophores to trace metal concentrations focused on *Emiliania huxleyi,* one of the most abundant species in the world ocean with a nearly global distribution (Westbroek et al., 1989; Winter et al., 2014). Experiments documented a decreasing growth rate under high trace metal concentrations (Vasconcelos et al., 2001; Hoffmann et al., 2012, Santomauro et al., 2016). So far, no such studies have been performed on other coccolithophore species. Furthermore, to our knowledge, this is the first study investigating the effect of high trace metal concentrations on coccolithophore and coccolith morphology and size. The trace metals tested (Zn, V, Ni, Pb) were chosen based on peaks identified in the geological record (Snow et al., 2005) and known trace metal interactions with living coccolithophores to simulate the environmental conditions during OAEs. The main goal of this study is to understand if, similarly to the fossil record, anomalously high quantities of essential and/or toxic metal induce changes in coccolith shape and size and cause coccolith dwarfism in coccolithophore species.

More specifically, we address the following questions: i) does coccolithophore growth change in response to increasing trace metal concentrations? ii) does coccolith size and morphology, as well as coccolithophore size, change in response to high and anomalous trace metal concentrations? iii) do trace metal combinations, which mimic OAEs conditions, lead to a uniform response among species or to species-specific responses on morphological features? iv) do coccolith morphometrical features have a potential to serve as a proxy to reconstruct paleo-ocean trace metal concentrations?

2 Material and Methods

2.1 Culture conditions

Monospecific cultures of the coccolithophores *Emiliania huxleyi* (strain RCC 1216)*, Gephyrocapsa oceanica* (strain RCC 1303)*, Coccolithus pelagicus* (strain PLY182G)*,* and *Pleurochrysis carterae* (no known strain number) were grown as batch cultures in artificial seawater (ASW) produced as described by Kester et al., (1967). The artificial seawater medium was enriched with 64 µmol kg^{-1} nitrate, 4 µmol kg^{-1} phosphate to avoid nutrient limitations, f/8 concentrations for vitamins (Guillard and Ryther, 1962), 10 nmol kg^{-1} of SeO_2 and 2 ml kg^{-1} of natural North Sea water (Bach et al., 2011). The carbonate chemistry was adjusted by bubbling with CO_2-enriched air overnight to reintroduce inorganic carbon thereby reaching atmospheric CO_2 partial pressure (~400 µatm). All culture bottles were manually and carefully rotated three times a day, each time with 20

3

rotations in order to avoid cell settling. In the control treatment, the medium was enriched with f/8 concentrations for trace metals (Guillard and Ryther, 1962).

Pb, Zn, Ni and V concentrations were added in low (L), medium (M), high (H) and extreme treatments because of their high concentrations identified in the Aptian OAE 1a (Erba et al., 2015) and Cenomanian-Turonian OAE 2 (Snow et al., 2005).

5 (Table 1). The trace metal chelator EDTA (ethylenediamine tetraacetic acid) was added to the trace metal stock solutions in order to guarantee a constant level of bioavailable trace metals for phytoplankton and prevent metal precipitation. The cultures were incubated in a thermo constant climate chamber (Rubarth Apparate GmbH) at a constant temperature of 15° C, a 16:8 [hour:hour] light/dark cycle, at a photon flux density of 150 µmol photons $m^{-2} s^{-1}$.

The cultures were pre-exposed to the different treatment conditions (acclimation period) for 7-10 generations, which varied

10 between 6-10 days depending on the species-specific cell division rates. All cultures were incubated in autoclaved 500 mL square glass bottles (Schott Duran). The initial cell density was relatively low with ~ 50 cells ml^{-1}. Final samples were taken when cells were still in their exponential growth phase and cell numbers were low enough to avoid a strong change in the chemical conditions of the growth medium. Therefore, the experimental duration differed among species and among treatments (between 6-10 days) due to the different growth rates. Each treatment was replicated three times. Final cell densities in the

15 experiment didn't exceed 50000 cells ml^{-1} in *E. huxleyi*, 20000 cells ml^{-1} in *G. oceanica,* and 3000 cells ml^{-1} in *C. pelagicus* and *P. carterae*.

2.2 Cell abundance and growth rate

Samples for cell abundance were taken every second day with the exception of the control treatment where samples were only

20 taken at the end of the experiment. Incubation bottles were gently turned 10 times in order to obtain a homogenous suspension of the cells before sampling. Cell numbers were immediately measured three times without addition of preservatives using a Beckman coulter Multisizer. Specific daily growth rates (µ) were calculated from the least-squares regression of cell counts versus time during exponential growth (Eq. 1)

25 $\mu = \frac{lnc1 - lnc0}{t1 - t0}$ (1)

were c0 and c1 are the cell concentrations at the beginning (t0) and at the end of the incubation period (t1), respectively.

2.3 Coccosphere and cell sizes

Cell abundance samples were acidified with 0.1 mmol L^{-1} HCl to dissolve all free and attached coccoliths and subsequently measured 3 times in order to obtain cell diameters and volumes (Müller et al., 2012). In this study, we define the coccosphere

30 volume as the coccolith-bearing cell volume, and the cell volume as the coccolith-free cell volume. Therefore, the volume of

the calcitic portion of the coccosphere (VCP) was estimated as:

Volume of the calcitic portion of the coccosphere (VCP) = coccosphere volume - cell volume

Coccolith volume and free coccolith concentrations were also determined for *C. pelagicus* (Fig. 1).

2.4 Coccolith dimensions and malformations

2.4.1 Scanning Electron Microscopy (SEM)

Samples were taken from each of the 48 incubation bottles. 5-10 ml of sample were filtered by gravity on polycarbonate filters (0.2 μm pore size) and dried directly after filtration at 60°C. Samples were sputtered with gold-palladium. SEM analysis was performed at the Earth Sciences department of the University of Milan with SEM Cambridge Stereoscope 360. For each sample, 50 specimens were digitally captured and subsequently analyzed with Image J software. All pictures were taken with the same magnification (5000x) and the scale bar given on SEM pictures was used for calibration (Fig 2).

2.4.2 Coccolith dimensions and *E. huxleyi* malformation

We measured the length of distal shield (DSL) and the width of the distal shield (DSW) manually using the public domain program Fiji distributed by ImageJ software (Schindelin et al., 2012). The distal shield area (DSA) was calculated, assuming an elliptical shape of the coccolith, as (Eq. 2):

$$DSA = \Pi \frac{DSL \ x \ DSW}{4} \quad (2)$$

Assuming elliptical shape has been shown to yield near identical results to direct measurements of DSA in *E. huxleyi* (Bach et al., 2012).

Malformations were determined for *E. huxleyi* since in the filters analyzed with SEM coccoliths were very abundant and allow a visual comparison of 100 individual coccoliths for every sample. We sorted the degree of malformation in several categories: our categories were used to describe the morphology of *E. huxleyi* as "normal", "malformed", "incomplete" and "incomplete and malformed" coccoliths (Langer et al., 2010; Langer et al., 2011) (for reference images for the categories, see Fig 3). We considered normal *E. huxleyi* coccolith with regular shape and well-formed distal shield elements forming a symmetric rim; malformed: malformed coccolith shape or malformed shape of individual elements; incomplete: coccolith with variations in its degree of completion; malformed and incomplete: coccolith with malformed shape and variations in its degree of completion.

2.5 Statistics

Prior to statistical analyses, data were tested for normality and homogeneity of variances. To test the null hypothesis the average value of parameters from triplicate cultures were compared between treatments. Mean μ values, coccosphere and cell diameters, VCP and coccolith sizes of each treatment were compared to the control and among each other. A one-way analysis of variance was used to determine statistical significance of the main effect of trace metals on the variables. A Tukey post-hoc test was used to identify the source of the main effect determined by ANOVA to assess whether differences in μ and sizes between trace metal treatments were statistically significant. Statistical treatments of data were performed using R software. Statistical significance was accepted for $p < 0.05$.

3 Results

3.1 Growth rate

In the treatment with extreme trace metal concentrations up to 8 μmol L^{-1}, none of the four species tested survived e the acclimation phase. In L, M and H treatments, however, *E. huxleyi*, *G. oceanica, C. pelagicus* and *P. carterae* all survived. However, the addition of trace metals decreased the growth rate of *E. huxleyi*, *G. oceanica,* and *C. pelagicus* compared to the control treatment. *E. huxleyi* growth rate was 1.22 d^{-1} in the controls and 1.12, 1.16 and 1.10 d^{-1} in L, M, H trace metal concentration treatments respectively (Table 2; Fig 4a). *G. oceanica* growth rate was 0.66 d^{-1} in the controls. In L, M and H the growth rate was significantly lower compared to the control at values of 0.58 d^{-1} in L, 0.60 d^{-1} in M and 0.58 d^{-1} in H. (Table 2; Fig 4b). *C. pelagicus* had an average growth rate in the control experiment of 0.56 d^{-1}. The growth rate was significantly lower in trace metal treatments compared to the control, with values of 0.42 d^{-1} in L and 0.43 d^{-1} in M and H is in average (Table 2; Fig 4c). Contrarily, *P. carterae* showed an increase in growth rate with trace metal addition compared to the control. In the control treatment, the growth rate was 0.52 d^{-1} and is significantly lower compared to L, M and H treatments with growth rates of 0.57, 0.56 and 0.57 d^{-1}, respectively (Table 2; Fig 4d).

3.2 Coccosphere and cell sizes and volume of the calcitic part of the coccosphere

In *E. huxleyi,* the mean coccosphere diameters were significantly lower in the L, M, and H treatments compared to the control (mean diameter 4.88 μm; Table 2, Fig 5a). The VCP was reduced under all increased trace metal treatments compared to the control conditions (Table 2; Fig 6a) with lowest VCP recorded in the M treatment.

In *G. oceanica,* the coccosphere diameters were largest in the control treatment (mean diameter 7.25 μm; Table 2; Fig 5b). L, M and H coccosphere diameters were significantly smaller compared to the control. Specifically, L and M show similar values of 6.58 μm and 6.60 μm, respectively, while H shows the lowest coccosphere diameter of 6.14 μm (Table 2). Similarly, cell

6

diameters were significantly larger in the control treatment (5.45 μm), intermediate in L and M (L= 5.18 μm; M=5.19 μm) and smaller in H (4.74 μm). Furthermore, the coccosphere and cell diameters were significantly smaller in H compared to L and M. The VCP was significantly reduced under increased trace metal concentrations compared to control conditions (Fig 6b) with similar coccosphere VCP recorded in both L, M and H.

5 *C. pelagicus* coccosphere and cell diameters were significantly larger in the control (19.82 μm and 15.65 μm, respectively) compared to L (17.12 μm and 10.10 μm, respectively), M (17.05 μm and 10.46 μm, respectively) and H (16.85 μm and 10.38 μm, respectively) (Table 2.; Fig 5c). However, a significant increase in coccosphere VCP was observed from 1760 in the control to 2102, 2036, and 1954 in the L, M and H treatments, respectively. (Fig 6c, Table 2).

P. carterae showed a smaller coccosphere diameter in the control compared to the L, M and H treatments. The coccosphere
10 diameter in L and H (L= 12.11 μm; H=11.99μm) is significantly bigger compared to the control (coccosphere diameter 11.70 μm). In M, the coccosphere has a mean diameter of M=11.88μm (Fig 5d). On the other hand, the cell diameters were very similar among all treatments. The VCP was slightly lower in the control compared to the other three treatments (L, M and H; Table 2.; Fig 6d).

3.3 Coccolith size and *C. pelagicus* coccolith concentrations

15 *E. huxleyi* coccoliths were longer and wider in the control treatment compared to the other three treatments (Table 3.). Increasing trace metal content reduced coccolith length and width significantly ($p < 0.05$) and the high trace metal treatment showed the lowest distal shield length (DSL) and distal shield width (DSW) coccolith size. In *G. oceanica* coccoliths were longer and wider in the controls compared to the other three treatments (Table 3). However only in H, coccolith were significantly smaller ($p < 0.05$) compared to the control treatment.

20 *C. pelagicus* coccoliths in the L, M and H trace metal treatments were significantly smaller compared to the control replicates (Table 3). Furthermore, a higher number of free coccoliths was present in the trace metal treatments compared to the control replicates (Table 4) and free coccoliths progressively increased with increasing trace metal content. *P. carterae* coccoliths showed very similar sizes in all the four treatments (Table 3).

3.4 *Emiliania huxleyi* coccolith malformation

25 Scanning electron microscope analyses of *E. huxleyi* coccoliths showed changes in the proportion of malformed and incomplete coccoliths. Specifically, malformations and incomplete coccoliths of *E. huxleyi* increased in all trace metal treatments (L, M and H concentrations) by about 20-35 % compared to the control treatment (Fig 7).

7

4 Discussion

4.1 Growth rate

Whereas in the extreme trace metal treatment none of the species survived the acclimation phase, revealing that the conditions were apparently poisonous in the L, M and H treatments the four test species responded in different ways to trace metal additions. Previous studies on *E. huxleyi* responses to trace metal enrichment resulting from volcanic ash showed no significant effects on growth rate for most ashes tested (Hoffmann et al., 2012). Only the addition of pumice, which released low concentration of trace metals, had a beneficial effect and increased *E. huxleyi* growth. In one case, however, progressively increased ash content strongly suppressed the growth rate of *E. huxleyi* in the volcanic ash which contained the highest trace metal concentrations (e.g. Pb from 0.5 up to 2.6 nM L^{-1}; Ni from 12 up to 60 nM L^{-1}) (Hoffmann et al., 2012). Vasconcelos et al. (2001), report a 10-20 % growth rate reduction of *E. huxleyi* with increasing Pb up to 0.25 µmol L^{-1} without additions of EDTA.

In our study, *E. huxleyi* growth decreased with increasing Pb, Zn, Ni, and V concentrations, whereby the highest concentration of trace metals up to 0.8 µmol L^{-1} slowed down *E. huxleyi* growth by 10% (Fig 4a). While *E. huxleyi* is a species which has been studied intensively, much less work has been done on other coccolithophore species. For example, trace metal effects on *G. oceanica* have not been tested before and in our experiments, we observed a decrease of *G. oceanica* growth of 12% under the highest trace metal concentrations (Fig 4b). A similar negative response to elevated trace metal concentration was observed for *C. pelagicus* where the growth rate decreased by 31% in each of the trace metal treatment compared to the control (Fig 4c). The bigger growth rate reduction observed for *C. pelagicus* suggests a comparatively high sensitivity of this species to trace metals enrichment. A stepwise increase in trace metal concentration did not induce any progressive growth rate reduction attesting a strong sensitivity of both *G. oceanica* and *C. pelagicus* already at low trace metal concentrations.

P. carterae growth rate generally increased with trace metal concentration (Fig 4d). This beneficial effect of high trace metal quantities (L, M and H) on *P. carterae* growth rate might be due to the preferred habitat of this species in eutrophic lagoons and estuaries (Heimdal, 1993), where trace metal concentrations are generally much higher (Sunda and Hunstman, 2005) than in open waters.

4.2 Morphometrical analyses

The coccolithophore species tested evidenced a detrimental effect of trace metals on coccosphere, cell and coccolith sizes. Indeed, three species, *E. huxleyi*, *G. oceanica* and *C. pelagicus,* displayed significant size reductions when grown under anomalously high trace metal concentrations. However, the morphometrical responses are highly variable among species (Fig 8): 1) *E. huxleyi* reduced its coccolith sizes under high trace metal concentration. This reduction can explain the coccosphere diameter decrease and the concomitant stable cell sizes. Additionally, an increase in the percentage of malformed and/or

incomplete coccoliths were observed under high trace metal concentrations. 2) Trace metal concentration also influenced *G. oceanica* coccosphere and cell sizes. Furthermore, an extra size reduction of both parameters, that goes along with coccolith size decrease, occurred at the highest trace metal concentration tested. This implies a particularly noxious effect of very high trace metal concentration on *G. oceanica* growth. 3) *C. pelagicus* coccosphere, cell diameters and coccolith sizes were negatively influenced by higher trace metal quantities. Increased trace metal induced a reduction of coccosphere, cell and coccolith sizes in *C. pelagicus* at all the concentrations tested. However, the volume of the calcitic portion of the coccosphere significantly increased under high trace metal concentrations. A plausible explanation is that the size decline of the cell goes hand in hand with an increase in the coccolith numbers that cover the cell. Indeed, progressively increased numbers of free/detached *C. pelagicus* coccoliths go together with a gradual increase in trace metal concentrations. (Table 4). This hints at a beneficial effect of trace metal on the number of *C. pelagicus* coccolith produced per cell (Paasche et al., 1998; Müller et al., 2012). 4) On the contrary*, P. carterae* doesn't show any sensitivity to trace metal concentration since coccosphere, cell and coccolith sizes remain stable in all treatments tested.

Coccolithophore algae therefore, respond differently to changes in trace metal concentrations. This species-specific sensitivity suggests a different degree of adaptation of the species tested.

4.3 Analogy and contrast with the fossil record

The trace metals tested here, were chosen based on metal peaks identified in the Aptian OAE 1a (Erba et al., 2015) and latest Cenomanian OAE 2 (Snow et al., 2005). Zn and Pb are more volatile elements that are concentrated in magmatically degassed fluids, while Ni and V are found in higher concentrations in water-rock exchange reactions of typical steady-state hydrothermal vents (Rubin, 1997). Therefore, the composure of trace metal tested was intended to simulate OAE conditions. We emphasize that the coccolithophore species chosen for this experiment are linked to the Mesozoic family Biscutaceae based on the fossil record tracing their biocalcification history back to ~200 million years ago (Bown et al., 2004). When genomic data-sets are considered for reconstruction of coccolithophore evolution, it appears that the selected Coccolithales order (*C. pelagicus* and *P. carterae*) diverged from the Isochrysidales order (*E. huxleyi* and *G. oceanica*) in the earliest Triassic (De Vargas et al., 2007) or even in the latest Permian (Liu et al., 2010), some 300 million years ago.

Considering that the species tested in this study have a long evolutionary history, it may be justified to conduct a comparison among fossil and living coccolithophore responses. Morphometric analyses of selected nannofossil taxa across Cretaceous OAEs in various geological settings, revealed differential species-specific patterns: for instance, *Biscutum constans*, a cosmopolitan coccolithophore species of the Cretaceous ocean, evidenced size variations in times of environmental change. Specifically, coccolith dwarfism (*sensu* Erba et al., 2010) occurred at intervals characterized by high trace metal concentrations (Erba et al., 2010; Erba et al., 2016; Faucher et al., 2017). Conversely, *Watzanaueria barnesiae*, a cosmopolitan species described as a r-selected opportunistic species (Hardas et al., 2007) did not change in size across OAEs (Erba et al., 2010; Bornemann and Mutterlose, 2006; Lübke and Mutterlose, 2016, Faucher et al., 2017). Indeed, a more pronounced ellipticity,

9

interpreted as evidence of malformation, was documented by Erba et al., (2010) during OAE 1a, but not during other times of global anoxia (Bornemann and Mutterlose, 2006; Faucher et al., 2017). The very low variability in *W. barnesiae* size indicates that this taxon was most adaptable and only marginally affected by the paleoenvironmental stress characterizing Cretaceous OAEs. Finally*, D. rotatorius* and *Z. erectus*, species with a meso-eutrophic preference, evidenced inconsistent size trends without a distinct relationship between size and metal peaks (Faucher et al., 2017).

Our laboratory experiments on living coccolithophore algae demonstrate that elevated trace metal concentrations affect coccolith size and/or weight similar to the fossil record. Moreover, as quantified in nannofossil assemblages, our results reveal species-specific responses. In fact, large differences were observed between species and we could identify the most- (*P. carterae*), intermediate- (*E. huxleyi, G. oceanica*), and the least- (*C. pelagicus*) tolerant taxa to increasing trace concentrations. Parallel changes among fossil and living coccolithophores suggest that trace metal concentrations have the potential to influence coccolith production and sizes.

We stress the fact that both the fossil record and the experimental results converge on a species-specific response of coccolithophores to metal availability. Consequently, the indiscriminate use of coccolith sizes as a proxy of trace metal concentration in seawater should be avoided. Instead, it is crucial to identify the species index/indices that better trace paleoenvironmental stress induced by high (selected) metal concentrations.

5 Conclusion

With this study, we demonstrated for the first time that a mixture of trace metals affected growth and morphology of all of the coccolithophore species. A size reduction of the coccosphere and cell diameters has been observed in three of the analyzed species. Furthermore, we observed the production of dwarf coccoliths (*sensu* Erba et al., 2010) under high trace metal concentrations. Our data show a species-specific sensitivity of coccolithophores to trace metal concentration, allowing the recognition of most- (*P. carterae*), intermediate- (*E. huxleyi* and *G. oceanica*), and least- (*C. pelagicus*) tolerant taxa.

The comparison of data on living coccolithophores and Mesozoic calcareous nannofossils shows strong similarities, suggesting that laboratory simulations of past extreme conditions are viable when extant taxa are phylogenetically linked to extinct fossil species. Our study supports the hypothesis that anomalous trace metal conditions in the past oceans significantly contributed to the morphological coccolith changes during Cretaceous OAEs.

Laboratory experiments on modern coccolithophore species remain the only means to quantitatively assess the individual or combined role of environmental parameters (e.g. trace metal availability) on coccolith secretion. Our results emphasize the need to consider species-specific differences where coccolith morphological features are used to reconstruct paleo-chemical conditions.

6 Acknowledgments

5 **References**

Bach, L. T., Riebesell, U., Schulz, K. G.: Distinguishing between the effects of ocean acidification and ocean carbonation in the coccolithophore Emiliania huxleyi. Limnology and Oceanography, 56(6), 2040-2050, 2011.

Bach, L. T., Bauke, C., Meier, K. J. S., Riebesell, U., & Schulz, K. G.: Influence of changing carbonate chemistry on morphology and weight of coccoliths formed by Emiliania huxleyi. Biogeosciences (BG), 9(8), 3449-3463, 2012.

10 Bornemann, A., Mutterlose, J.: Size analyses of the coccolith species *Biscutum constans* and *Watznaueria barnesiae* from the Late Albian "Niveau Breistroffer" (SE France): taxonomic and palaeoecological implications. Geobios 39(5) 599-615, 2006.

Bown, P. R., Lees, J. A., Young, J. R.: Calcareous nannoplankton evolution and diversity through time. In *Coccolithophores* (pp. 481-508). Springer Berlin Heidelberg, 2004.

Bruland, K. W., Donut, J.R., Hutchins, D. A.: Interactive influences of bioactive trace metals on biological production in 15 oceanic waters. Limnol. Oceanogr, 36(8), 1555-1577, 1991.

De Vargas, C., Probert, I.: New keys to the Past: Current and future DNA studies in Coccolithophores. Micropaleontology, 45-54, 2004.

De Vargas, C., Aubry, M., P., Probert, I., and Young, J.: Origin and evolution of coccolithophores: from coastal hunters to 20 oceanic farmers. Evolution of primary producers in the sea, 12, 251-285, 2007.

Erba E (2004) Calcareous nannofossils and Mesozoic oceanic anoxic events. Marine Micropaleontology, 52, 1, 85-106, doi:10.1016/j.marmicro.2004.04.007, 2004.

Erba, E., Bottini, C., Weissert, H. J., Keller, C. E.: Calcareous nannoplankton response to surface-water acidification around Oceanic Anoxic Event 1a. Science, 329(5990), 428-432, doi: 10.1126/science.1188886, 2010.

25 Erba E, Duncan RA, Bottini C, Tiraboschi D, Weissert H, Jenkyns HC et al.: Environmental Consequences of Ontong Java Plateau and Kerguelen Plateau Volcanism. GSA Special Paper 511 doi:10.1130/2015.2511, 2015.

Faucher, G., Erba, E., Bottini, C., Gambacorta, G.: Calcareous nannoplankton response to the latest Cenomanian Oceanic Anoxic Event 2 perturbation. Rivista italiana di paleontologia e stratigrafia (research in paleontology and stratigraphy), 123(1), 2017.

30 Guillard, R. R. L., Ryther, J. H.: Studies of marine planktonic diatoms: I. Cyclotella Nana Hustedt, and Detonula Confervacea (CLEVE) Gran." Canadian journal of microbiology 8.2: 229-239, 1962.

11

Hardas, P., Mutterlose, J.: Calcareous nannofossil assemblages of Oceanic Anoxic Event 2 in the equatorial Atlantic: Evidence of an eutrophication event. Marine Micropaleontology 66(1) 52-69, http://dx.doi.org/10.1016/j.marmicro.2007.07.007, 2007.

Heimdal, B. R.: Modern coccolithophorids. CR Tomas. Academic Press, San Diego, CA, 731-831, 1993

Hoffmann, L. J., Breitbarth, E., Ardelan, M. V., Duggen, S., Olgun, N., Hasellöv, M., Wängberg, S. Å.: Influence of trace metal release from volcanic ash on growth of *Thalassiosira pseudonana* and *Emiliania huxleyi*. Marine Chemistry 132 28-33., 2012.

Jenkyns, H.C.: Geochemistry of oceanic anoxic events. Geochemistry, Geophysics Geosystems 11 Q03004 doi:10.1029/2009GC002788, 2010.

Kester, D. R., Duedall, I. W., Connors, D. N., Pytkowicz, R. M.: Preparation of artificial seawater. Limnology and oceanography 12(1) 176-179, 1967.

Langer, G., De Nooijer, L. J., Oetjen, K.: On the role of the cytoskeleton in coccolith morphogenesis: the effect of cytoskeleton inhibitors1. Journal of Phycology 46(6) 1252-1256 doi: 0.1111/j.1529-8817.2010.00916.x, 2010.

Langer, G., Bode, M.: CO_2 mediation of adverse effects of seawater acidification in Calcidiscus leptoporus. Geochemistry, Geophysics, Geosystems, 12(5) doi:10.1029/2010GC003393, 2011.

Larson, R. L. and Erba, E.: Onset of the Mid-Cretaceous greenhouse in the Barremian-Aptian: igneous events and the biological, sedimentary, and geochemical responses. Paleoceanography, 14(6), 663-678, doi:10.1029/1999PA900040, 1999.

Leckie, R. M.: Foraminifera of the Cenomanian-Turonian Boundary Interval, Greenhorn Formation, Rock Canyon Anticline, Pueblo, Colorado. In: Society of Economic Paleontologists and Mineralogists Field Trip Guidebook 4, 139-155. Midyear Meeting, Golden, Colorado, 1985.

Leckie, R. M., Yuretich, R. F., West, O. L. O., Finkelstein, D., Schmidt, M.: Paleoceanography of the southwestern Western Interior Sea during the time of the Cenomanian-Turonian boundary (Late Cretaceous), in Stratigraphy and Paleoenvironments of the Cretaceous Western Interior Seaway, USA, Concepts in Sedimentol. Paleontol. vol. 6, edited by Dean WE and Arthur MA pp. 101–126, Soc. Sediment. Geol., Tulsa, Okla, 1998.

Liu, H., Aris-Brosou, S., Probert, I., and de Vargas, C.: A time line of the environmental genetics of the haptophytes. *Molecular biology and evolution*, *27*(1), 161-176, https://doi.org/10.1093/molbev/msp222, 2010.

Lübke, N. and Mutterlose, J.: The impact of OAE 1a on marine biota deciphered by size variations of coccoliths. *Cretaceous Research*, *61*, 169-179, 2016.

Müller, M. N., Beaufort, L., Bernard, O., Pedrotti, M. L., Talec, A., Sciandra, A.: Influence of CO_2 and nitrogen limitation on the coccolith volume of *Emiliania huxleyi* (Haptophyta). Biogeosciences (BG) 9(10) 4155-4167, 2012.

Neal, C. R., Coffin, M. F., Arndt, N. T., Duncan, R. A., Eldholm, O., Erba, E., et al. (2008). Investigating large igneous province formation and associated paleoenvironmental events: a white paper for scientific drilling. Scientific Drilling, 6, 4-18, 2008.

Orth, C. J., Attrep, M., Quintana, L. R., Elder, W. P., Kauffman, E. G., Diner, Villamil, T.: Elemental abundance anomalies in the late Cenomanian extinction interval: a search for the source(s). Earth and Planetary Science Letters 117(1) 189-204, 1993.

12

Paasche, E.: Roles of nitrogen and phosphorus in coccolith formation in *Emiliania huxleyi* (Prymnesiophyceae). European Journal of Phycology 33(1) 33-42, 1998.

Pearce, M. A., Jarvis, I., Tocher, B. A.: The Cenomanian–Turonian boundary event, OAE2 and palaeoenvironmental change in epicontinental seas: new insights from the dinocyst and geochemical records. Palaeogeography, Palaeoclimatology, Palaeoecology 280(1) 207-234, 2009.

Rubin, K.: Degassing of metals and metalloids from erupting seamount and mid-ocean ridge volcanoes: observations and predictions. Geochimica et Cosmochimica Acta 61(17) 3525-3542, 1997.

Santomauro, G., Sun, W. L, Brümmer, F., Bill, J: Incorporation of zinc into the coccoliths of the microalga *Emiliania huxleyi.* BioMetals 29(2) 225-234 doi: 10.1007/s10534-015-9908-y, 2016.

Schindelin, J., Arganda-Carreras, I., Frise, E., Kaynig, V., Longair, M., Pietzsch, T., Rueden, C., Saalfeld, S., Schmid, B., Tinevez, J., Y., White, D. J., Hartenstein, V., Eliceiri K., Tomancak, P. and Cardona, A.: Fiji: an open-source platform for biological-image analysis. Nature methods, 9(7), 676-682, doi:10.1038/nmeth.2019, 2012.

Snow, L. J., Duncan, R. A., Bralower, T.J.: Trace element abundances in the Rock Canyon Anticline, Pueblo, Colorado, marine sedimentary section and their relationship to Caribbean plateau construction and oxygen anoxic event 2. Paleoceanography doi:10.1029/2004PA001093, 20, 3., 2005.

Sunda, W.G., Huntsman, S.A.: Processes regulating cellular metal accumulation and physiological effects: phytoplankton as model systems. Science of the Total Environment 219(2) 165-181, 1998.

Vasconcelos, M. T. S., Leal, M. F. C.: Antagonistic interactions of Pb and Cd on Cu uptake, growth inhibition and chelator release in the marine algae Emiliania huxleyi. Marine Chemistry 75(1) 123-139, 2001.

Winter, A., Henderiks, J., Beaufort, L., Rickaby, R. E., & Brown, C. W.: Poleward expansion of the coccolithophore Emiliania huxleyi. Journal of Plankton Research, 36(2), 316-325, 2014.
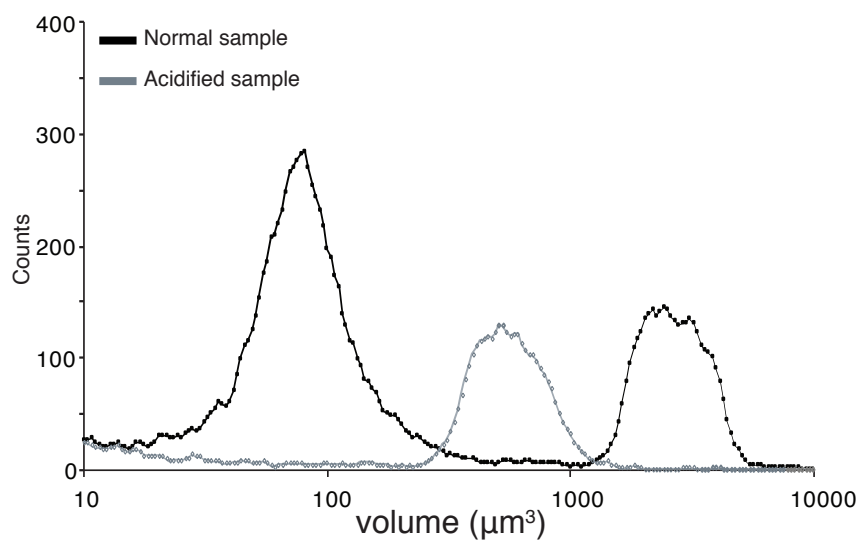
Figure 1: Example of multisizer volume spectra. Black line: spectra of *C. pelagicus* population (coccolith spectrum and coccosphere spectrum); grey line*: C. pelagicus* coccolith-free cell after treatment with HCl.
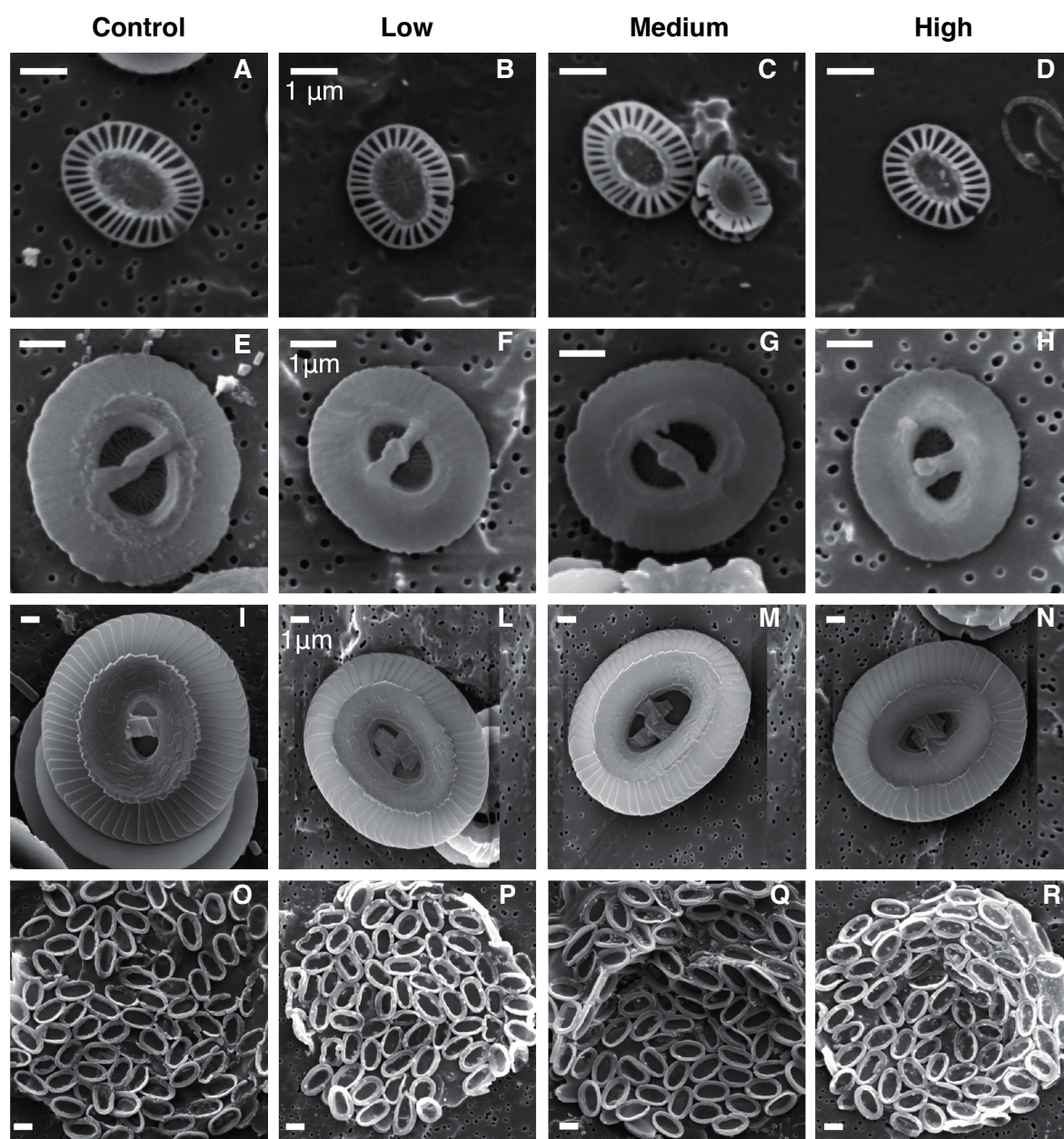
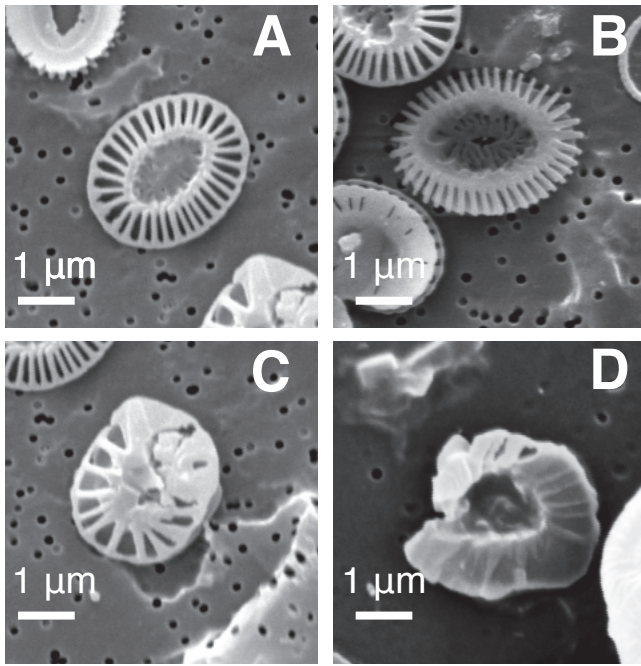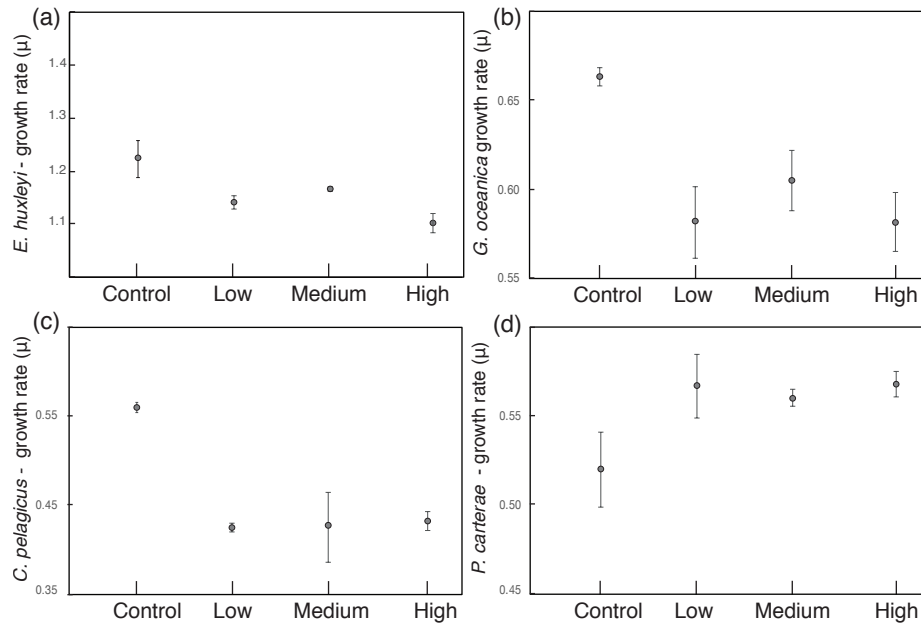| Control | Low | Medium | High |

Figure 2: Plate. Example of the coccoliths of the four species tested under different trace metal concentrations. A-D, *E. huxleyi***; E-H,** *G. oceanica***; I-L,** *C. pelagicus***; M-P,** *P. carterae.*

15

Figure 3: SEM images of *Emiliania huxleyi* coccoliths. A. Normal coccolith; B. Incomplete coccolith; C. Malformed coccolith; D. Malformed and incomplete coccolith.

Figure 4: Average growth rate; all measurements are done in triplicates; error bars denote standard deviation. If not visible, error bars are smaller than symbols. A) *E. huxleyi;* **B)** *G. oceanica;* **C)** *C. pelagicus;* **D)** *P. carterae.* **Note the different scales on the y-axis.**

5

17
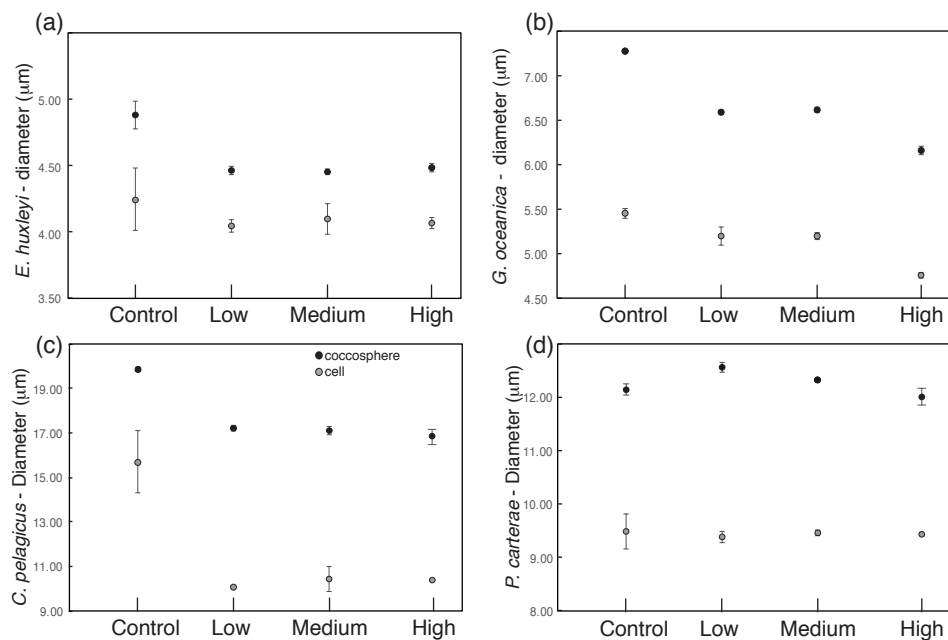
Figure 5: Average values of the coccolithophore diameters (black dots) and cell diameters (grey dots). All measurements were done in triplicates, error bars denote standard deviation. If not visible, error bars are smaller than symbols. A) *E. huxleyi;* B) *G. oceanica*; C) *C. pelagicus*; D) *P. carterae.* **Note the different scales on the y-axis.**

5
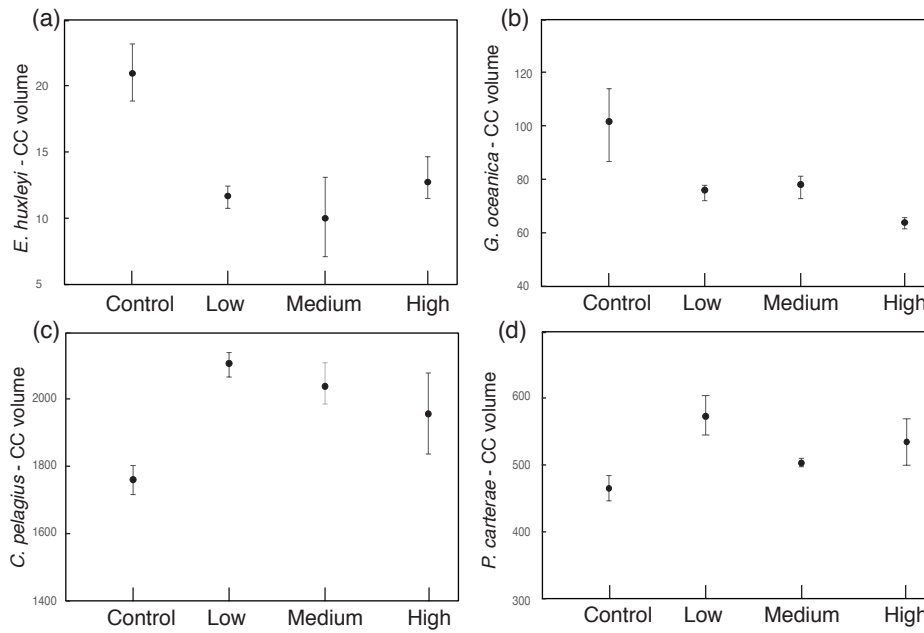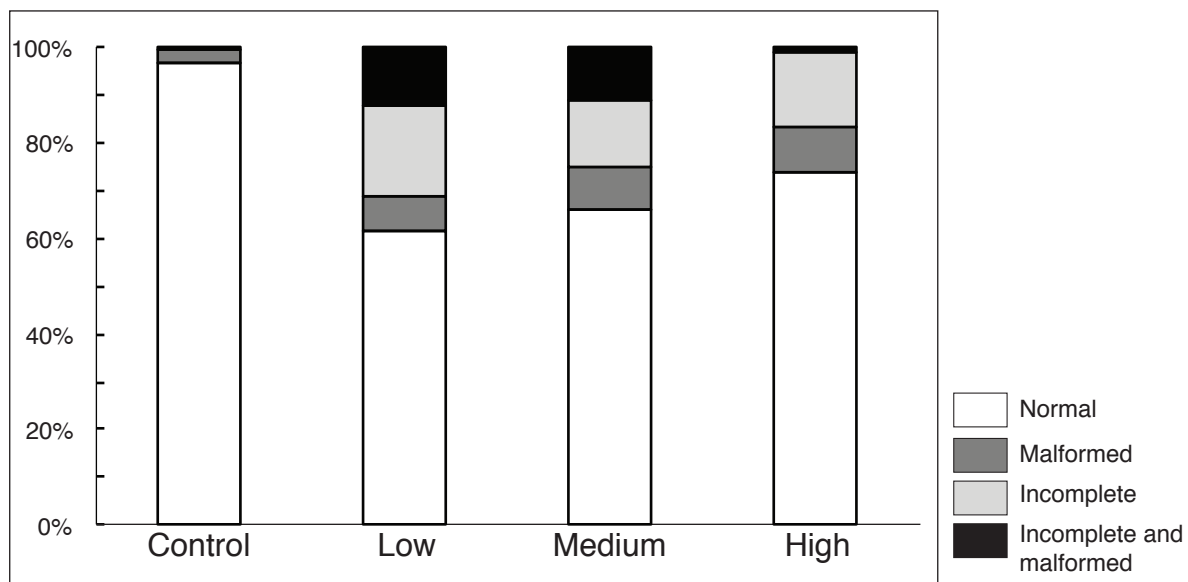
10

15

18

Figure 6: Average volume of the calcitic portion of the coccosphere (VCP). All measurements were done in triplicates; error bars denote standard deviation. If not visible, error bars are smaller than symbols measured for each replicate: A) *E. huxleyi;* **B)** *G. oceanica***; C)** *C. pelagicus***; D)** *P. carterae.* **Note the different scales on the y-axis.**

5

10

15

20

19

Figure 7: Malformation percentage. Percentages of normal, malformed, incomplete and malformed and incomplete coccoliths of *E. huxleyi* versus trace metal concentrations.

5

10

15

20

25

A
E.huxleyi
L - M - H

reduced coccosphere diameter

= cell diameter

small coccolith

B
G. oceanica
L - M

reduced coccosphere diameter

reduced cell diameter

= coccolith size

Control treatment

coccosphere

cell

C
G. oceanica
H

reduced coccosphere diameter

reduced cell diameter

small coccolith

D
C. pelagicus
L - M - H

reduced coccosphere diameter

reduced cell diameter

small coccolith
increased number of coccolith per cell

Figure 8: Species-specific responses to trace metal enrichment

5

	Control	Low	Medium	High	Extreme
	μmol $^{L-1}$				
$FeCl_3 \cdot 6H_2O$	11.7	11.7	11.7	11.7	11.7
$Na_2 \cdot 2H_2O$	11.7	11.7	11.7	11.7	11.7
$CuSO_4 \cdot 5H_2O$	0.04	0.04	0.04	0.04	0.04
$Na_2MoO4 \cdot 2H_2O$	0.03	0.03	0.03	0.03	0.03
$CoCl_2 \cdot 6H_2O$	0.04	0.04	0.04	0.04	0.04
$ZnSO_4 \cdot 7H_2O$	0.08	0.16	0.16	0.96	8.08
Pb	………	0.01	0.08	0.8	8.00
$NiCl_2 \cdot 6H_2O$	………	0.08	0.08	0.8	8.00
$VOSO_4$	………	0.08	0.08	0.8	8.00
EDTA	11.7	11.7	11.7	11.7	11.7

Table 1. Trace metal concentrations in the growth medium of the different treatments.

5

10

15

20

25

30

	E. huxleyi				G. oceanica			
	Control	Low	Medium	High	Control	Low	Medium	High
μ	1.22	1.12*	1.16	1.10*	0.66	0.58*	0.60*	0.58*
Coccosphere D	4.88	4.45*	4.44*	4.48*	7.25	6.58*	6.60*	6.14*
Cell D	4.22	4.04	4.08	4.05	5.45	5.18*	5.19*	4.74*
VCP	20.98	11.78*	10.01*	12.83*	101.02	75.48*	77.41*	62.96*
	C. pelagicus				P. carterae			
	Control	Low	Medium	High	Control	Low	Medium	High
μ	0.56	0.42*	0.43*	0.43*	0.52	0.57*	0.56*	0.57*
Coccosphere D	19.82	17.12*	17.05*	16.85*	11.70	12.11*	11.88	11.99*
Cell D	15.65	10.10*	10.46*	10.38*	9.03	8.93	9.02	8.98
VCP	1760	2102*	2036*	1954*	463	570*	500	533*

Table 2. μ = growth rate, coccosphere D (μm) = coccosphere diameter, cell D = cell diameters (μm) and VCP = volume of the calcitic portion of the coccosphere (μm^3). Significance was tested using an ANOVA and a Tukey post-hoc test ($p < 0.05$). Asterisks indicate significant difference from the control treatment.

	Control			Low			Medium			High		
	DSL	DSW	DSA	DSL	DSW	DSA	DSL	DSW	DSA	DSL	DSW	DSA
E. huxleyi	2.98	2.44	5.71	2.66*	2.11*	4.42	2.65*	2.06*	4.29	2.59*	1.98*	4.03
G. oceanica	4.31	3.77	12.78	4.10	3.57	11.47	4.15	3.58	11.69	3.97*	3.37*	10.49
C. pelagicus	12.76	11.08	111.08	10.43*	8.43*	69.11	10.03*	8.17*	64.38	10.47*	8.50*	69.87
P. carterae	1.90	1.18	1.75	1.68	1.05	1.38	1.87	1.16	1.70	1.90	1.19	1.78

Table 3. Coccolith distal shield length (DSL, µm) and distal shield width (DSW; µm) average values and calculated distal shield area (DSA; μm^2) for all experiments. Asterisks indicate significant difference from the control treatment. Significance of DSL and DSW was tested using an ANOVA and a Tukey post-hoc test ($p < 0.05$). Asterisks indicate significant difference from the control treatment

	replicate	free coccolith number		replicate	free coccolith number
Control	r1	2112	**Medium**	r1	9017
	r2	2297		r2	10046
	r3	2972		r3	12325
Low	r1	8876	**High**	r1	13089
	r2	7734		r2	11523
	r3	8358		r3	11350

Table 4. Free *C. pelagicus* coccolith concentration measured with the coulter counter; r= replicates.